Numerical Simulation of Polarized Light and Temperature in a Stratified Atmosphere with a Slowly Varying Refractive Index

Olivier Pironneau

Numerical Simulation of Polarized Light and Temperature in a Stratified Atmosphere with a Slowly Varying Refractive Index

Olivier Pironneau[1]

Abstract

This article aims to elucidate the effect of a slowly varying refractive index on the temperature in a stratified atmosphere, with a particular focus on greenhouse gases such as CO_2. It validates an iterative method called iterations on the source but it shows also that the system proposed by Chandrasekhar and Pomraning requires compatibility conditions when the refractive index varies. So instead we solve the integral representation of the Vector Radiative Transfer Equations (VRTE) in which the unphysical ray directions have been removed. Some mathematical proofs are given showing monotonicity of the iterations and some numerical tests showing the effect of a layer of cloud with a refracting index greater than air, polarisation and Rayleigh scattering.

Keywords: Radiative transfer, Polarization, Integral equation, Numerical analysis, Climate modeling MSC classification 3510, 35Q35, 35Q85, 80A21, 80M10

Contents

[1] *olivier.pironneau@sorbonne-universite.fr* , LJLL, Sorbonne Université, Paris, France.

Introduction

The investigation of polarized light in a stratified or plane parallel atmosphere not only provides crucial insights into the dynamics of light propagation and polarization within complex atmospheric environments but also holds significant implications for understanding the impact of greenhouse gases on the Earth's climate system in the presence of clouds [2]. Building upon the Vector Radiative Transport Equation (VRTE), as established by the seminal works of Chandrasekhar [3] and Pomraning [12] later, this article aims to elucidate the effect of the refractive index on the temperature with a particular focus on the greenhouse gas (GHG) such as CO_2.
Varying concentrations of greenhouse gases are modelled by their effects on absorption and scattering in given ranges of frequencies. The study shows that the numerical method is capable of reproducing small changes due to GHG and the influence of refraction from clouds.
Clouds have a refracting index close to air and varying smoothly, unlike an air/water interface for which the Fresnel laws need to be applied (see [5] and [8] for a numerical implementation).
The computer graphics community has used VRTE with varying refractive indices for realistic rendering (see L.H. Liu [9], Ament et al [1] and the references therein). But most of their numerical implementation assume a given temperature field.
Temperature variations are at the core of the present study; the partial differential equations of VRTE are converted into a set of integral equations using the method of characteristics. Iterations on the sources are used together with Newton iterations on the temperature equations. Convergence and monotony are analyzed. However total refraction of some rays has to be dealt with.

This approach can be generalized in 3D (non stratified atmospheres) as in [6], [11].
The equations analysed in [10] and their integral formulations are extended to refracting atmospheres. New difficulties arise, which are problematic: the characteristic curves may not cross the boundaries where light source is given, leading to an ill-posed problem, and exponential integrals cannot be used which makes the computer implementation more difficult and less precise.

1. Fundamental Equations

In classical physics, light in a medium Ω is an electromagnetic radiation satisfying Maxwell's equations. The electric field $\mathbf{E}$ of a monochromatic plane wave of frequency ν propagating in direction $\mathbf{k}$, $\mathbf{E} = \mathbf{E_0}\exp(\mathrm{i}(\mathbf{k}\cdot\mathbf{x} - \nu t))$, is a solution to Maxwell equations which is suitable to describe the propagation of a ray of light for which ν is very large.
Such radiations are characterized by their Stokes vector $\mathbf{I}$, made of the irradiance I and 3 functions Q, U, V to define the state of polarization. The radiation source $\mathbf{F}$ for an unpolarized-emitting black-body is given by the Planck function $B_\nu(T) = \nu^3(\mathrm{e}^{\frac{\nu}{T}} - 1)^{-1}$. The scalings used in this article are defined in [7]. If $\mathbf{E_0}$ is written in polar coordinates,

$$\mathbf{I} := \begin{bmatrix} I \\ Q \\ U \\ V \end{bmatrix} = \frac{1}{2}\sqrt{\frac{\epsilon_0}{\mu_0}} \begin{bmatrix} E_{0\theta}E_{0\theta}^* + E_{0\phi}E_{0\phi}^* \\ E_{0\theta}E_{0\theta}^* - E_{0\phi}E_{0\phi}^* \\ E_{0\theta}E_{0\phi}^* - E_{0\phi}E_{0\theta}^* \\ E_{0\phi}E_{0\theta}^* - E_{0\theta}E_{0\phi}^* \end{bmatrix} \qquad \mathbf{F} := \begin{bmatrix} \kappa_a B_\nu(T) \\ 0 \\ 0 \\ 0 \end{bmatrix},$$

where ϵ_0 and μ_0 are the electric and magnetic permeability of the medium. The parameter κ_a is related to absorption and scattering (see (2.3) below). which, by the way, are quantum effects, not described by Maxwell's equations. Using $\mathbf{I}$ rather than $\mathbf{E}_0$ one models absorption and scattering by a system of partial differential equations (PDE), known as VRTE [12] p152; with $\tilde{\mathbf{I}} := \mathbf{I}/n^2$,

$$\frac{n}{c}\partial_t\tilde{\mathbf{I}} + \boldsymbol{\omega}\nabla_{\mathbf{x}}\tilde{\mathbf{I}} + \frac{\nabla_{\mathbf{x}} n}{n}\cdot\nabla_{\boldsymbol{\omega}}\tilde{\mathbf{I}} + \kappa\tilde{\mathbf{I}} = \int_{\mathbb{S}_2}\mathbb{Z}(\mathbf{x},\boldsymbol{\omega}' : \boldsymbol{\omega})\tilde{\mathbf{I}}\mathrm{d}\omega' + \frac{\mathbf{F}}{n^2}, \tag{1.1}$$

for all $\mathbf{x} \in \Omega, \boldsymbol{\omega} \in \mathbb{S}_2$, where c is the speed of light, n the refractive index of the medium , $\mathbb{S}_2$ the unit sphere, κ the absorption and $\mathbb{Z}$ is the phase scattering matrix for rays $\boldsymbol{\omega}'$ scattered in direction $\boldsymbol{\omega}$ and $\mathbf{F}$ is the volumic source term (for example due to the black-body radiation of air). It is assumed that n

depends (weekly) only on position $\mathbf{x} \in \Omega$; κ depends on $\mathbf{x}$ and strongly on ν. Because c is very large, the term $\frac{1}{c}\partial_t \mathbf{I}$ is neglected. Thermal equilibrium is assumed:

$$\nabla_{\mathbf{x}} \cdot \int_{\mathbb{R}_+} \int_{\mathbb{S}_2} \tilde{I} \boldsymbol{\omega} \mathrm{d}\omega \mathrm{d}\nu = 0. \tag{1.2}$$

Notation 1. *On all variables, the tilde indicates a division by n^2. Arguments of functions are sometimes written as indices like κ_ν and n_z.*

Following [9], given a cartesian frame $\mathbf{i}, \mathbf{j}, \mathbf{k}$, the third term on the left in (1.1) is computed in polar coordinates, with

$$\boldsymbol{\omega} := \mathbf{i} \sin\theta \cos\varphi + \mathbf{j} \sin\theta \sin\varphi + \mathbf{k} \cos\theta, \quad \mathbf{s}_1 := -\mathbf{i} \sin\varphi + \mathbf{j} \cos\varphi,$$

$$\nabla_{\mathbf{x}} \log n \cdot \nabla_{\boldsymbol{\omega}} \tilde{\mathbf{I}} = \frac{1}{\sin\theta} \frac{\partial}{\partial\theta} \left\{ \tilde{\mathbf{I}} (\cos\theta \boldsymbol{\omega} - \boldsymbol{k}) \cdot \nabla_{\mathbf{x}} \log n \right\} + \frac{1}{\sin\theta} \frac{\partial}{\partial\varphi} \left\{ \tilde{\mathbf{I}} \ \boldsymbol{s}_1 \cdot \nabla_{\mathbf{x}} \log n \right\}.$$

When n does not depend on x, y but only on z, it simplifies to

$$\nabla_{\mathbf{x}} \log n \cdot \nabla_{\boldsymbol{\omega}} \tilde{\mathbf{I}} = (\partial_z \log n \cdot) \partial_\mu \left\{ (1 - \mu^2) \tilde{\mathbf{I}} \right\} \quad \text{where } \mu = \cos\theta.$$

2. The Stratified Case

The general expression of the phase matrix for Rayleigh scattering according to S. Chandrasekhar [3] is given in Appendix 7.

For an atmosphere of thickness Z over a flat ground, the domain is $\Omega = \mathbb{R}^2 \times \times (0, Z)$, and all variables are independent of x, y. In [3], p40-53, expressions for the phase matrix $\mathbb{Z}$ are given for Rayleigh and isotropic scattering for the φ-averaged of I and Q,

$$\bar{I} := \frac{1}{2\pi} \int_0^{2\pi} I \mathrm{d}\varphi, \quad \bar{Q} := \frac{1}{2\pi} \int_0^{2\pi} Q \mathrm{d}\varphi,$$
$$\bar{\mathbb{Z}}_R = \frac{3}{2} \begin{bmatrix} 2(1 - \mu^2)(1 - \mu'^2) + \mu^2 \mu'^2 & \mu^2 \\ \mu'^2 & 1 \end{bmatrix} \quad \bar{\mathbb{Z}}_I = \frac{1}{2} \begin{bmatrix} 1 & 1 \\ 1 & 1 \end{bmatrix}$$

For a given $\beta \in [0, 1]$, we shall consider a combination of $\beta \mathbb{Z}_R$ (Rayleigh scattering) plus $(1 - \beta) \mathbb{Z}_I$ (isotropic scatterings) [3],[12],[13]. As it is understood that no variables are φ dependent, we drop the overline.

The two other components of the Stokes vectors have autonomous equations,

$$\mu \partial_z \tilde{U} + \partial_z \log n \cdot \partial_\mu \{ (1 - \mu^2) \tilde{U} \} + \kappa \tilde{U} = 0, \tag{2.1}$$

$$\mu \partial_z \tilde{V} + \partial_z \log n \cdot \partial_\mu \{ (1 - \mu^2) \tilde{V} \} + \kappa \tilde{V} = \frac{\mu}{2} \int_{-1}^{1} \mu' \tilde{V}(z, \mu') \mathrm{d}\mu'. \tag{2.2}$$

Notation 2. *Denote the scattering coefficient $a_s \in [0,1)$, which, as κ, is a function of altitude z and frequency ν. Define*

$$\kappa_s = \kappa a_s, \qquad \kappa_a = \kappa - \kappa_s = \kappa(1 - a_s). \tag{2.3}$$

From (2.1),(2.2) we see that, if the light source at the boundary is unpolarized then $U = V = 0$ and the light can be described either by I and Q or two orthogonal components I_l, I_r, such that $I = I_l + I_r$ and $Q = I_l - I_r$:

$$\begin{aligned}
&\mu\partial_z \tilde I_l + \partial_z \log n \cdot \partial_\mu\{(1-\mu^2)\tilde I_l\} + \kappa \tilde I_l \\
&\qquad = \frac{3\beta\kappa_s}{8}\int_{-1}^{1}([2(1-\mu'^2)(1-\mu^2) + \mu'^2\mu^2]\tilde I_l + \mu^2 \tilde I_r)\mathrm{d}\mu' \\
&\qquad + \frac{(1-\beta)\kappa_s}{4}\int_{-1}^{1}[\tilde I_l + \tilde I_r]\mathrm{d}\mu' + \frac{\kappa_a}{2}\tilde B_\nu(T(z)), \\
&\mu\partial_z \tilde I_r + \partial_z \log n \cdot \partial_\mu\{(1-\mu^2)\tilde I_r\} + \kappa \tilde I_r + \frac{3\beta\kappa_s}{8}\int_{-1}^{1}\mu'^2(\tilde I_l + \tilde I_r)\mathrm{d}\mu' \\
&\qquad + \frac{(1-\beta)\kappa_s}{4}\int_{-1}^{1}[\tilde I_l + \tilde I_r]\mathrm{d}\mu' + \frac{\kappa_a}{2}\tilde B_\nu(T(z)),
\end{aligned} \tag{2.4}$$

Using an appropriate linear combination of (2.4), the system for $\tilde I$ and $\tilde Q$ is derived,

$$\begin{aligned}
&\mu\partial_z \tilde I + \partial_z \log n \cdot \partial_\mu\{(1-\mu^2)\tilde I\} + \kappa \tilde I \\
&\qquad = \kappa_a \tilde B_\nu + \frac{\kappa_s}{2}\int_{-1}^{1}\tilde I \mathrm{d}\mu' + \frac{\beta\kappa_s}{4}P_2(\mu)\int_{-1}^{1}[P_2 \tilde I - (1-P_2)\tilde Q]\mathrm{d}\mu', \\
&\mu\partial_z \tilde Q + \partial_z \log n \cdot \partial_\mu\{(1-\mu^2)\tilde Q\} + \kappa \tilde Q \\
&\qquad = -\frac{\beta\kappa_s}{4}(1-P_2(\mu))\int_{-1}^{1}[P_2 \tilde I - (1-P_2)\tilde Q]\mathrm{d}\mu',
\end{aligned} \tag{2.5}$$

where $P_2(\mu) = \frac{1}{2}(3\mu^2 - 1)$. The temperature $T(z)$ is linked to I by (1.2) which, in the case of (2.5) is as follows.

Proposition 1. *Thermal equilibrium for* (2.4) *or* (2.5) *is*

$$\int_{\mathbb{R}_+}\kappa_a\big[\tilde B_\nu(T) - \tfrac{1}{2}\int_{-1}^{1}\tilde I\, d\mu\big]d\nu = 0. \tag{2.6}$$

Proof Averaging in μ the first equation of (2.5) leads to

$$\begin{aligned}
\nabla_{\mathbf{x}} \cdot \int_{\mathbb{S}_2}\boldsymbol{\omega}\tilde I = \partial_z\Big(\frac{1}{2}\int_{-1}^{1}\mu \tilde I \mathrm{d}\mu\Big) &= -\frac{1}{2}\partial_z \log n \cdot \int_{-1}^{1}\partial_\mu\{(1-\mu^2)\tilde I\}\mathrm{d}\mu - \frac{1}{2}\kappa\int_{-1}^{1}\tilde I \mathrm{d}\mu \\
&+ \frac{1}{2}\int_{-1}^{1}\kappa_a \tilde B_\nu \mathrm{d}\mu + \frac{\kappa_s}{2}\int_{-1}^{1}\tilde I \mathrm{d}\mu',
\end{aligned}$$

because $\int_{-1}^{1}P_2(\mu)\mathrm{d}\mu = 0$. Now the first term on the right integrates to zero and $\kappa - \kappa_s = \kappa_a$. □

2.1. Iterative Solution

Consider the following iterations,

$$\begin{aligned}
&\mu\partial_z \tilde{I}_l^{n+1} + \partial_z \log n \cdot \partial_\mu\{(1-\mu^2)\tilde{I}_i^{n+1}\} + \kappa \tilde{I}_l^{n+1} \\
&\quad = \frac{3\beta\kappa_s}{8}\int_{-1}^{1}([2(1-\mu'^2)(1-\mu^2)+\mu'^2\mu^2]\tilde{I}_l^n + \mu^2\tilde{I}_r^n)\mathrm{d}\mu' \\
&\qquad\qquad + \frac{(1-\beta)\kappa_s}{4}\int_{-1}^{1}[\tilde{I}_l^n + \tilde{I}_r^n]\mathrm{d}\mu' + \frac{\kappa_a}{2}\tilde{B}_\nu^n \\
&\mu\partial_z \tilde{I}_r^{n+1} + \partial_z \log n \cdot \partial_\mu\{(1-\mu^2)\tilde{I}_r^{n+1}\} + \kappa \tilde{I}_r^{n+1} \\
&\quad = \frac{3\beta\kappa_s}{8}\int_{-1}^{1}(\mu'^2\tilde{I}_l^n + \tilde{I}_r^n)\mathrm{d}\mu' + \frac{(1-\beta)\kappa_s}{4}\int_{-1}^{1}[\tilde{I}_l^n + \tilde{I}_r^n]\mathrm{d}\mu' + \frac{\kappa_a}{2}\tilde{B}_\nu^n \\
&\int_{\mathbb{R}_+}\kappa_a \tilde{B}_\nu(T^{n+1})\mathrm{d}\nu = \int_{\mathbb{R}_+}\kappa_a\left(\frac{1}{2}\int_{-1}^{1}(\tilde{I}_l^n + \tilde{I}_r^n)\mathrm{d}\mu\right)\mathrm{d}\nu \quad \forall z.
\end{aligned} \tag{2.7}$$

2.2. The Method of Characteristics

By analogy with the non-refracting case we write the transport equations above as a 2-system for $\tilde{\mathbf{I}} := [\tilde{I}_l^{n+1}, \tilde{I}_r^{n+1}]^T$,

$$\partial_z \tilde{\mathbf{I}} + \frac{1-\mu^2}{\mu}\partial_z \log n \cdot \partial_\mu \tilde{\mathbf{I}} + \frac{\kappa}{\mu}\tilde{\mathbf{I}} = \frac{1}{\mu}\tilde{\mathbf{S}}(\mu, z), \tag{2.8}$$

where $\tilde{\mathbf{S}} = \mathbf{S}_0 + \mu^2\tilde{\mathbf{S}}_2$ and the $\mathbf{S}_k$ are linear combinations of $\int_{-1}^{1}\mathbf{I}^n \mathrm{d}\mu'$ and $\int_{-1}^{1}\mu'^2\mathbf{I}^n\mathrm{d}\mu'$. The characteristic curves are given by

$$\dot{z} = 1, \quad \dot{\mu}\mu = (1-\mu^2)\partial_z \log n \Rightarrow z(s) = s + z_0, \quad \mu^2(s) = 1 - (1-\mu_0^2)\frac{n_0^2}{n^2(z(s))} \tag{2.9}$$

Then (2.8) is

$$\frac{\mathrm{d}\tilde{\mathbf{I}}}{\mathrm{d}s} + \frac{\kappa(z(s))}{\mu(s)}\tilde{\mathbf{I}} = \frac{1}{\mu(s)}\tilde{\mathbf{S}}(\mu(s), z(s))$$

Compatible boundary conditions are : $\tilde{\mathbf{I}}(z_0, \mu_0)$ given for $\mu_0 > 0$ (resp. < 0) at all $z_0 \in \partial\Omega$ where the outer normal of $\partial\Omega$ points downward (resp. upward). For clarity assume that $z_0 = 0$ and $\tilde{\mathbf{I}}$ is given at $z = 0$ for all $\mu > 0$. Denote $\kappa(s) = \kappa(z(s))$. Then the solution is

$$\begin{aligned}
\tilde{\mathbf{I}}(z(s), \mu(s)) = \mathbf{1}_{\mu_0>0}&\left[\mathrm{e}^{-\int_0^s \frac{\kappa(s')}{\mu(s')}ds'}\tilde{\mathbf{I}}(0, \mu_0) + \int_0^s \frac{\mathrm{e}^{-\int_{s'}^{s}\frac{\kappa(s'')}{\mu(s'')}ds''}}{\mu(s')}\tilde{\mathbf{S}}(s')\mathrm{d}s'\right] \\
&- \mathbf{1}_{\mu_0<0}\left[\int_s^S \frac{\mathrm{e}^{\int_s^{s'}\frac{\kappa(s'')}{\mu(s'')}ds''}}{\mu(s')}\tilde{\mathbf{S}}(s', \mu(s'))\mathrm{d}s'\right].
\end{aligned} \tag{2.10}$$

where S is such that $(z(S),\mu(S))$ is the exit point of the characteristic.

2.3. Compatible Characteristics

Obviously (2.10) hols only if there is an exit point $z(S)=Z$. In other words for every altitude z^* and direction μ^* there must exist a characteristic $\{z(s),\mu(s)\}_0^S$ and a $\mu_0>0$ such that for some s^* $\{z(s^*)=z^*,\mu(s^*)=\mu^*\}$ and $z(0)=0,\mu(0)=\mu_0$. Otherwise the problem is ill-posed! By (2.9), with $z_0=0$, the direction $\mu^2<1-\frac{n_0^2}{n_z^2}$ is forbidden at z. Note that

$$
\begin{aligned}
&\mu^2(z)>1-\frac{n_0^2}{n_z^2},\quad \mu^2(z')=1-(1-\mu^2(z))\frac{n_z^2}{n_{z'}^2}\implies\\
&\mu^2(z')>1-\frac{n_z^2}{n_{z'}^2}+(1-\frac{n_0^2}{n_z^2})\frac{n_z^2}{n_{z'}^2}>1-\frac{n_0^2}{n_{z'}^2}.
\end{aligned}
$$

Consequently, if $\mu(s)$ is admissible in (2.10), $\mu(s')$ and $\mu(s'')$ are computable. Note that if $z\mapsto n(z)$ is decreasing, $\mu\in(-1,1)$ is always admissible and (2.8), with $\tilde{\mathbf{I}}$ given at $z=0$ for $\mu>0$, is well posed.

Proposition 2. *Assume that the light source is given at altitude zero:*

$$
\tilde{\mathbf{I}}(0,\mu_0)=\tilde{\mathbf{P}}\mu_0,\ \textit{with}\ \mathbf{P}=[c_E B_\nu(T_E),0,0,0]^T,\ \textit{for some given}\ c_E,T_E.
$$

Then the solution of (2.8) *exists and is unique for all* $z>0,\mu\geq\left((1-\frac{n_0^2}{n_z^2})^+\right)^{\frac{1}{2}}$.

Consequently the end points of the characteristics are such that $z(0)=0,z(S)=Z$ and z can be used in place of s. Hence,

$$
\begin{aligned}
\tilde{\mathbf{J}}_0(z)\coloneqq\frac{1}{2}\int_{-1}^1\tilde{\mathbf{I}}(z,\mu)\mathrm{d}\mu=\frac{1}{2}\tilde{\mathbf{P}}\int_0^1 &\mathrm{e}^{-\int_0^z\frac{\kappa(z')}{\mu(z')}dz'}\mu_0\mathrm{d}\mu\\
&+\int_0^Z\left(\int_0^1\mathrm{e}^{-\int_{z'}^z\frac{\kappa(z'')}{\mu(z'')}dz''}\mu^{-1}(z')\mathrm{d}\mu\right)\tilde{\mathbf{S}}_0(z')\mathrm{d}z'\\
&+\int_0^Z\left(\int_0^1\mathrm{e}^{-\int_{z'}^z\frac{\kappa(z'')}{\mu(z'')}dz''}\mu(z')\mathrm{d}\mu\right)\tilde{\mathbf{S}}_2(z')\mathrm{d}z'
\end{aligned}
$$

By (2.9) with

$$
\bar{\mu}(\mu,z,z')\coloneqq\left(1-(1-\mu^2)\frac{n_{z'}^2}{n_z^2}\right)^{\frac{1}{2}}\quad\forall z',z''\in[0,Z], \tag{2.11}
$$

$$
\mu_0=\bar{\mu}(\mu,z,0),\quad \mu(z')=\bar{\mu}(\mu,z,z'),\quad \mu(z'')=\bar{\mu}(\mu,z,z'') \tag{2.12}
$$

It can be applied with $z' = 0$ and $z'' = z$ to compute $\mu_0 = \bar{\mu}(\mu(z), z, 0)$ and to compute the first integral in μ above together with $\mu(z') = \bar{\mu}(\mu(z), z, z')$. For the last integral $\mu(z'')$ and $\mu(z')$ must be similarly expressed in terms of $\mu(z)$.

Remark 1. *Note that $\bar{\mu}$ could be imaginary, which violates the hypothesis on the end points of the characteristics. These values are not be included in the computations that follow. As explained in [5]-eq.(31), it happens when the critical refraction angle is reached. The above handles refracted rays but makes no room for reflected rays.*

Proposition 3. *By analogy with exponential integrals, let us define $\{\mathbb{E}_k\}_{k\geq 1}$ and write, for $z' < z$, $u > 0$*

$$\mathbb{E}_k(u, z, z') := \int_{\mu^*}^{1} \mathrm{e}^{-\int_{z'}^{z} \frac{u(z'')}{\mu(z'')} dz''} \mu^{k-2}(z') d\mu, \quad \mu^* = \left((1 - \frac{n_0^2}{n_z^2})^+\right)^{\frac{1}{2}}$$

$$= \int_{\mu^*}^{1} \mathrm{e}^{-\int_{z'}^{z} \frac{u(z'')}{\bar{\mu}(\mu, z, z'')} dz''} \bar{\mu}^{k-2}(\mu, z, z') d\mu, \ \bar{\mu} \textit{ given by } (2.11) \quad (2.13)$$

$$\tilde{\mathbf{J}}_0(z) = \frac{c_E}{2} \tilde{B}_\nu(T_E) \mathbb{E}_3(\kappa, z, 0) + \sum_{k=1,3} \int_0^Z \mathbb{E}_k(\kappa, z, z') \tilde{\mathbf{S}}_{k-1}(z') dz' \quad (2.14)$$

Note that if $z \to n(z)$ is decreasing, $\mu^* = 0$.

3. Convergence of the Iterations on the Source

3.1. Monotony

First notice that $T \to B_\nu(T)$ is monotone in the sense that $T^n \geq T'^n$ implies $\tilde{B}_\nu(T^n) \geq \tilde{B}_\nu(T'^n)$. Then observe that, all coefficients being positive, $\tilde{I}^n_{l,r} \geq \tilde{I}'^n_{l,r}$ implies that $\tilde{I}^{n+1}_{l,r} \geq \tilde{I}'^{n+1}_{l,r}$. More precisely, subtract (2.7) for $\tilde{I}'^{n+1}_{l,r}$ from (2.7) for $\tilde{I}^{n+1}_{l,r}$ and check that it is an equation for the difference $D^{n+1}_{l,r} := \tilde{I}^{n+1}_{l,r} - \tilde{I}'^{n+1}_{l,r}$ with positive source,

$$\begin{aligned}
\mu\partial_z D_l^{n+1} &+ \partial_z \log n \cdot \partial_\mu\{(1-\mu^2) D_l^{n+1}]\} + \kappa D_l^{n+1} \\
&= \frac{3\beta\kappa_s}{8} \int_{-1}^{1} ([2(1-\mu'^2)(1-\mu^2) + \mu'^2\mu^2] D_l^n + \mu^2 D_r^n) \mathrm{d}\mu' \\
&+ \frac{(1-\beta)\kappa_s}{4} \int_{-1}^{1} [D_l^n + D_r^n] \mathrm{d}\mu' + \frac{\kappa_a}{2} [\tilde{B}_\nu(T'^n) - \tilde{B}_\nu(T^n)] \\
\mu\partial_z D_r^{n+1} &+ \partial_z \log n \cdot \partial_\mu\{(1-\mu^2) D_r^{n+1}\} + \kappa D_r^{n+1} \\
&= \frac{3\beta\kappa_s}{8} \int_{-1}^{1} (\mu'^2 D_l^n + D_r^n) \mathrm{d}\mu'
\end{aligned}$$

$$+\frac{(1-\beta)\kappa_s}{4}\int_{-1}^{1}[D_l^n+D_r^n]\mathrm{d}\mu'+\frac{\kappa_a}{2}[\tilde B_\nu(T'^n)-\tilde B_\nu(T^n)]$$

Finally the last equation of (2.7) implies

$$\begin{aligned}\int_{\mathbb{R}_+}\kappa_a\tilde B_\nu(T'^{n+1})\mathrm{d}\nu &= \int_{\mathbb{R}_+}\kappa_a\left(\tfrac12\int_{-1}^{1}(\tilde I'^n_l+\tilde I'^n_r)\mathrm{d}\mu\right)\\ &\ge \int_{\mathbb{R}_+}\kappa_a\left(\tfrac12\int_{-1}^{1}(\tilde I^n_l+\tilde I^n_r)\mathrm{d}\mu\right)=\int_{\mathbb{R}_+}\kappa_a\tilde B_\nu(T'^{n+1})\mathrm{d}\nu\end{aligned}$$

which implies that $T^{n+1}\ge T'^{n+1}$. Let us apply this argument to $\{T^{n-1},\tilde I^{n-1}_{i,r}\}$ instead of $\{T'^n,\tilde I'^n_{i,r}\}$. It shows that

$$T^n\ge T^{n-1},\ \tilde I^n_{l,r}\ge\tilde I^{n-1}_{i,r}\quad\Rightarrow\quad T^{n+1}\ge T^n,\ \tilde I^{n+1}_{l,r}\ge\tilde I^n_{i,r}.$$

To start the iterations appropriately, simply set $T^0=0$, $\tilde I^0_{l,r}=0$, then by the positivity of the coefficients $\tilde I^1_{l,r}\ge 0$ and $T^1\ge 0$.

The same argument works with $T^n\le T'^n$, $\tilde I^n_{l,r}\le\tilde I'^n_{l,r}$ implying that $\tilde I^{n+1}_{l,r}\le\tilde I'^{n+1}_{l,r}$ and then $T^{n+1}\le T'^{n+1}$. Hence starting with $T^1<T^0$, $\tilde I^1_{l,r}\le\tilde I^0_{l,r}$ leads to a decreasing sequence toward the solution. For the scalar model, it is shown that it suffices to take $T^0(z)>T_M,\forall z$ where T_M is the solution of $B_\nu(T_M)=P_E B_\nu(T_E)$. For the present vector model it is not clear that it is sufficient.

The above results are summarized in the following theorem.

Proposition 4. *If the solution $T^*,I^*_{l,r}$ of (2.4)(2.6) exists (or equivalently (2.5)(2.6)), it can be reached numerically from above or below by iterations (2.7) and these are monotone increasing and decreasing respectively.*

The convergence is probably superlinear. Uniqueness may also be proved as in [7].

3.2. Boundedness

The following is an informal argument to show that boundedness for all $z\in(\epsilon,Z)$, $\epsilon<<1$ is likely true but probably false on $(0,\epsilon)$.

Denote $\tilde I^{n+1}=\tilde I^{n+1}_l+\tilde I^{n+1}_r$ and let

$$\tilde J^m_0(z):=\tfrac12\int_{-1}^{1}\tilde I^m\mathrm{d}\mu,\quad m=n+1,n.$$

By adding the first two equations of (2.7), the system leads to

$$\mu(s)\frac{\mathrm{d}\tilde I^{n+1}}{\mathrm{d}s}+\kappa(s)\tilde I^{n+1}\le\kappa_a\tilde B^n_\nu+(\frac14\beta+\frac12)\kappa_s\tilde J^n_0,\quad\forall\mu,z,\nu,$$

$$\int_{\mathbb{R}_+}\kappa_a\tilde{B}_\nu(T^{n+1})\mathrm{d}\nu=\int_{\mathbb{R}_+}\kappa_a\tilde{J}_0^{n+1}\mathrm{d}\nu\quad\forall z.$$

because $2(1-\mu^2)(1-\mu'^2)+\mu^2\mu'^2+\mu'^2\le 2$. By Hypothesis 2 (2.10) becomes

$$\tilde{I}(z(s),\mu(s))\quad=\mathrm{e}^{-\int_0^s\frac{\kappa(s')}{\mu(s')}ds'}c_E\mu_0\tilde{B}_\nu(T_E)+\int_0^Z\frac{\mathrm{e}^{-\int_{s'}^s\frac{\kappa(s'')}{\mu(s'')}ds''}}{\mu(s')}\tilde{S}(s')\mathrm{d}s'$$

and

$$\tilde{S}\le\kappa_a\tilde{B}^n+(\frac{5\beta}{4}+1)\kappa_s\tilde{J}_0^n.$$

Therefore, an integration in μ leads to

$$\tilde{J}_0^{n+1}(z)\le\frac{c_E}{2}\mathbb{E}_3(\kappa,0,z)\tilde{B}_\nu(T_E)+\int_0^Z\tfrac{1}{2}\mathbb{E}_1(\kappa,z,y)(\kappa_a\tilde{B}^n+(\frac{5\beta}{4}+1)\kappa_s\tilde{J}_0^n)\mathrm{d}y.$$

where $\mathbb{E}_3$ and $\mathbb{E}_1$ are defined (2.13). Multiply the above by κ_a and integrate in z and ν,

$$\begin{aligned}\int_0^Z\int_{\mathbb{R}_+}\kappa_a\tilde{J}_0^{n+1}\mathrm{d}\nu\mathrm{d}z\le\int_0^Z\int_{\mathbb{R}_+}\kappa_a(z)\frac{c_E}{2}\mathbb{E}_3(\kappa,0,z)\tilde{B}_\nu(T_E)\mathrm{d}\nu\mathrm{d}z\\+\int_{\mathbb{R}_+}\int_0^Z\int_0^Z\tfrac{1}{2}\kappa_a(z)\mathbb{E}_1(\kappa,z,y)\mathrm{d}z\Big(\kappa_a(y)\tilde{B}^n(y)\\+(\frac{5\beta(y)}{4}+1)\kappa_s(y)\tilde{J}_0^n(y)\Big)\mathrm{d}y\mathrm{d}\nu.\end{aligned}$$

When n is constant it was shown in [7] that

$$\tfrac{1}{2}\sup_{0\le y\le Z}\int_0^Z\mathbb{E}_1(\kappa,z,y)\kappa\mathrm{d}z\le C_1(\kappa)<1,\quad E_3\le\frac{1}{2}E_1.$$

For simplicity, assume that $z\to n(z)$ is increasing and very close to $n(0)$. Then we can try to extend this inequality by continuity by computing $\frac{\mathrm{d}\mathbb{E}}{\mathrm{d}N}|_{N=1}$ where $N=\frac{n_z^2}{n_{z'}^2}$ and use a Taylor expansion; for some N^*, from (2.13)

$$\mathbb{E}_1(\kappa,z,z')|_N=\mathbb{E}_1(\kappa,z,z')|_{N=1}+\frac{\mathrm{d}\mathbb{E}_1}{\mathrm{d}N}|_{N^*}(N-1)=E_1(|\int_{z'}^z\kappa|)+\frac{\mathrm{d}\mathbb{E}_1}{\mathrm{d}N}|_{N^*}(N-1).$$

$$\begin{aligned}\frac{\mathrm{d}\mathbb{E}_1}{\mathrm{d}N}|_{N=1}=\frac{1}{2}\Big(E_0(|\int_{z'}^z u|)-E_{-2}(|\int_{z'}^z u|)\Big)|\int_{z'}^z u|\\-\frac{1}{2}E_{-1}(|\int_{z'}^z u|)+\frac{1}{2}E_1(|\int_{z'}^z u|).\end{aligned}$$

with E_k being the exponential integrals,

$$E_k(v):=\int_0^1\mu^{k-2}\mathrm{e}^{-\frac{v}{\mu}}\mathrm{d}\mu,\ k\ge 1.\quad E_{k-1}(v)=\frac{\mathrm{e}^{-v}}{v}-\frac{k}{v}E_k(v),\ k\le 1,\ v\ne 0.$$

Unfortunately $E_{-1}(v)$ and $vE_{-2}(v)$ are unbounded near $v = 0$ (the 2 other terms are bounded). Hence the boundedness argument of [10] can be extended only for $|\int_{z'}^{z} u| \geq c^* > 0$ and $|\frac{n_{z'}^2}{n_z^2} - 1| << 1$. Then for some $C_\epsilon = 2\max_{z>\epsilon}\frac{\mathrm{d}\mathbb{E}}{\mathrm{d}N}$, assume that the data are such that $\eta < 1$,

$$\eta := C_1(\kappa_M)\frac{1-a_m}{1-a_M}(1+\frac{1}{2}\beta_M a_M) + C_2\max_{z,z'}|n(z)-n(z')| < 1,$$
$$H^{n+1} := \int_\epsilon^Z \int_{\mathbb{R}_+} \kappa_a \tilde{J}_0^{n+1}\mathrm{d}\nu\mathrm{d}z \leq C_1(\kappa_M)(1-a_m)\int_{\mathbb{R}_+}\frac{c_E}{2}B(T_E)\mathrm{d}\nu + \eta H^n,$$

It implies that H^n is bounded. In turn, all variables being positive, it implies that J^n, B^n, T^n are bounded too provided their definition are altered by replacing the integrals on $(0,Z)$ by integrals on (ϵ, Z).

4. Implementation with Integrals

Consider (2.5), the system for the irradiance I and the polarization Q. Denote

$$\tilde{J}_k(z) = \tfrac{1}{2}\int_{-1}^{1}\mu^k\tilde{I}\mathrm{d}\mu \quad \tilde{K}_k(z) = \tfrac{1}{2}\int_{-1}^{1}\mu^k\tilde{Q}\mathrm{d}\mu. \quad k = 0, 2.$$

Then (2.5) is rewritten as

$$\begin{aligned}
\mu\partial_z\tilde{I} + \partial_z\log n\cdot\partial_\mu\{(1-\mu^2)\tilde{I}\} + \kappa\tilde{I} &= \kappa_a\tilde{B}_\nu + \kappa_s\tilde{J}_0 \\
&\quad + \frac{\beta\kappa_s}{4}P_2(\mu)(3\tilde{J}_2 - \tilde{J}_0 - 3\tilde{K}_0 + 3\tilde{K}_2) \\
\mu\partial_z\tilde{Q} + \partial_z\log n\cdot\partial_\mu\{(1-\mu^2)\tilde{Q}\} + \kappa\tilde{Q} &= \\
&\quad - \frac{\beta\kappa_s}{4}(1-P_2(\mu))(3\tilde{J}_2 - \tilde{J}_0 - 3\tilde{K}_0 + 3\tilde{K}_2)
\end{aligned}$$

Let these be multiplied by μ^k and integrated in μ. By (2.14)

$$\begin{aligned}
\tilde{J}_k(z) &= \tfrac{1}{2}\int_{-1}^{1}\mu^k\tilde{I}(z,\mu)\mathrm{d}\mu = \frac{c_E}{2}\tilde{B}_\nu(T_E)\mathbb{E}_{k+3}(\kappa,z,0) \\
&+\frac{1}{2}\int_0^Z\left(\mathbb{E}_{k+1}(\kappa,z,y)S_0(y) + \mathbb{E}_{k+3}(\kappa,z,y)S_2(y)\right)\mathrm{d}y.
\end{aligned}$$

with

$$S_0 = \kappa_a\tilde{B} + \kappa_s\tilde{J}_0 - \frac{3\beta\kappa_s}{8}(\tilde{J}_2 - \tfrac{1}{3}\tilde{J}_0 - \tilde{K}_0 + \tilde{K}_2) \quad S_2 = \frac{9\beta\kappa_s}{8}(\tilde{J}_2 - \tfrac{1}{3}\tilde{J}_0 - \tilde{K}_0 + \tilde{K}_2).$$

Similarly (recall that $\tilde{Q}$ is zero at $z=0$),

$$\tilde{K}_k(z) = \tfrac{1}{2}\int_0^Z \left(\mathbb{E}_{k+1}(\kappa,z,y)S_0'(y) + \mathbb{E}_{k+3}(\kappa,z,y)S_2'(y)\right)\mathrm{d}y,$$

with

$$S_0' = \frac{9\beta\kappa_s}{8}(\tilde{J}_2 - \tfrac{1}{3}\tilde{J}_0 - \tilde{K}_0 + \tilde{K}_2) \quad S_2' = -\frac{9\beta\kappa_s}{8}(\tilde{J}_2 - \tfrac{1}{3}\tilde{J}_0 - \tilde{K}_0 + \tilde{K}_2).$$

So at each iteration we only need to compute, for $k=0,2$,

$$\tilde{H}_k(\nu,z) := \tfrac{9}{16}\int_0^Z \mathbb{E}_{k+1}(\kappa,z,z')\beta\kappa_s[\tilde{J}_2(z') - \tfrac{1}{3}\tilde{J}_0(z') - \tilde{K}_0(z') + \tilde{K}_2(z')]\mathrm{d}z',$$

and then set

$$\begin{aligned}\tilde{J}_k(z) \quad &= \tfrac{1}{2}\tilde{B}_\nu(T_E)\mathbb{E}_{k+3}(\kappa,z,0) + \tfrac{1}{2}\int_0^Z \mathbb{E}_{k+1}(\kappa,z,z')(\kappa_a\tilde{B} + \kappa_s\tilde{J}_0)\mathrm{d}z' \\ &-\frac{1}{3}\tilde{H}_k + \tilde{H}_{k+2}, \qquad \tilde{K}_p(z) = \tilde{H}_k - \tilde{H}_{k+2},\end{aligned}$$

and update T by solving

$$\int_{\mathbb{R}} \kappa_a(B_\nu(T(z)) - J_0(z,\nu))\mathrm{d}\nu = 0, \quad \forall z \in (0,Z)$$

5. An approximation to use Exponential Integrals

Assume that $n_{z'}^2 = n_z^2(1+\epsilon)$, $\epsilon << 1$. Then $\mu^2(z') = \bar{\mu}(\mu(z)) = (1+\epsilon)\mu^2(z) - \epsilon$. The computer implementation is easier and fast if the last ϵ dropped, i.e.

$$\mu'(z') = \mu(z)\frac{n_{z'}}{n_z} \approx \mu(z)(1+\frac{\epsilon}{2}), \tag{5.1}$$

because then exponential integrals can be used to approximate $\mathbb{E}_k$ deffined in (2.13). Figure 1 shows the error between $\mu(z')$ and $\mu'(z')$.
Indeed, if E_k is the k^{th} exponential integral,

$$\mathbb{E}_k(u,z,z') \approx \left(\frac{n_{z'}}{n_z}\right)^{k-2} E_k(\int_{z'}^{z} u(z'')\frac{n_z}{n_{z''}}\mathrm{d}z''). \tag{5.2}$$

However Figure 2 shows that this approximation is much too course for $\mathbb{E}_1$ but feasible for $\mathbb{E}_3$ and $\mathbb{E}_5$.
To optimize the computing time, $\mathbb{E}$ is tabulated in an array for 100 values of z, z' and 50 values of κ_ν. Computing this array takes 5" and the rest of the prograam runs faster than with E_1.

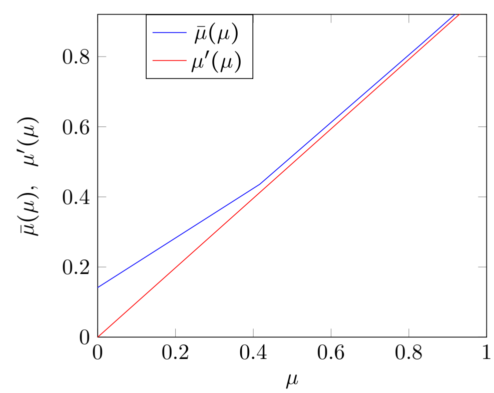

Figure 1: Difference between $\mu'(\mu)$ and $\bar{\mu}(\mu)$ (see (5.1)) when $n_{z'}/n_z = 0.99$.

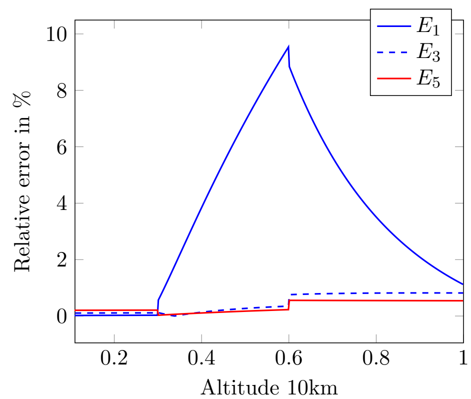

Figure 2: Relative error due to (5.2) for $\mathbb{E}_k$, $k = 1, 3, 5$ when n_z is as in §5.1.

5.1. Numerical Results

According to [2] the variation of the refractive index in the atmosphere is quite small ~ 0.003. To enhance the efffect we use 3 times this value.
For all the test the following is used:

- $n(z) = 1 + \epsilon \frac{(z-\frac{Z}{3})(\frac{Z}{2}-z)}{\max[(z-\frac{Z}{3})(\frac{Z}{2}-z)]} \mathbf{1}_{z\in(\frac{Z}{3},\frac{Z}{2})}$,
- $a_s = a_1 \mathbf{1}_{z\in(z_1,z_2)} + a_2 \mathbf{1}_{z>z_2} \mathbf{1}_{\nu\in(\nu_1,\nu_2)} \left(\frac{\nu}{\nu_2}\right)^4$,
- $\epsilon = 0.01,\ a_1 = 0.7,\ a_2 = 0.3,\ z_1 = 0.4,\ z_2 = 0.8,\ \nu_1 = 0.6,\ \nu_2 = 1.5$.

The monotony of the iterative process is displayed in Figure 4. It is clear that by starting below (resp. above) the solution the values of the temperature at $z = 300$m are increasing (resp. decreasing). Note that 15 iterations are sufficient to obtain a 3 digit precision.
To study the effect of n on a simple case with ran the program with $\kappa = 0.5$, n as in 5.1 and $n = 1$ and the data of Case 1. The results are shown in Figures 5 and 6. In all other test cases κ is the function of ν extracted from the Gemini experiments [2]. In Figure 7 Temperature versus altitude is displayed for Case 1 & 2 for 2 different $\nu \to \kappa$, the Gemini values and the Gemini $\nu \to \kappa_1$ modified due to an increase of CO_2 as shown in Figure 3. The main points are

[2] www.gemini.edu/observing/telescopes-and-sites/sites#Transmission

- For Case 1 (IR light coming from Earth) the CO_2 increases the temperature from 23.8 to 24.2 at the surface and from -52.8 to -51.5 at $z = 10$km.
- For Case 2 (Visible light coming from the sun and reflected by the Earth) the effect of the CO_2 is a drastic reduction of temperature.
- In both cases the influence of the cloud is seen as an inflection in the temperature.

In Figure 8, with κ-Gemini, the integrals of intensities over all ray directions are shown, namely $\nu \to J_0$ and the polarization $\nu \to K_0$ at ground and 10km levels. J_0 increases with altitude while K_0 decreases. As $10^7 K_0(Z)$ has large negative values at some points we have displayed $\tilde{K}_0 = \max(K_0, -2\,10^{-6})$.
In Figure 8 and 10 the effect of adding an added opacity in the range $14 - 18\mu$m is seen very strongly on $K_0(0)$.
Notice that the polarization is particularly strong at ground level near $\nu = \frac{3}{18}$ and since $Q(0,\mu) = 0$ when $\mu > 0$ it is entirely due to rays pointing downward.

.

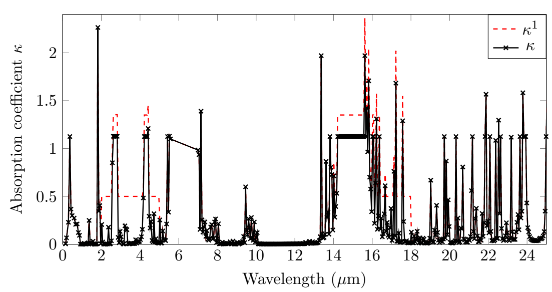

Figure 3: Absorption κ from the Gemini experiment, versus wavenumber ($3/\nu$). In dotted lines, the modification to construct κ_1 to account for the opacity of CO_2.

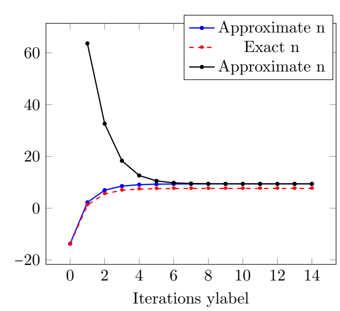

Figure 4: Convergence of the temperature at altitude 300m during the iterations. In solid line when it is started with $T^0 = 0$, in dashed line when it intial temperature is 180°C. Notice the monotonicity of both curves.

.

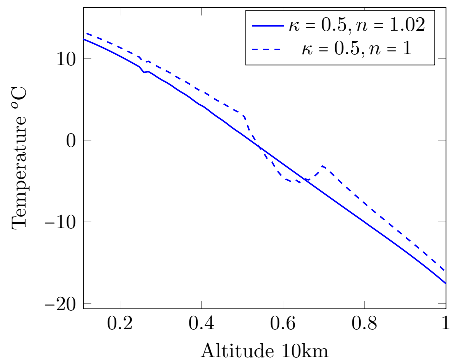

Figure 5: **Case 1**. Temperatures versus altitude The dashed curve is computed with $\kappa 0.5, n = 1$. The solid curve is computed with $\kappa 0.5$, n as in 5.1.

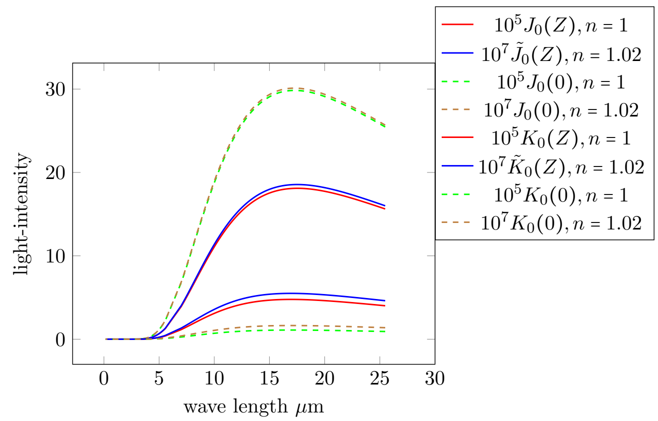

Figure 6: **Case 1**. Total light intensity J_0 and polarized K_0 versus wave length at ground level and altitude Z=10km.

6. Conclusion

In this article the methodology developed in (Golse-Pironneau (2022)[7]) for the numerical solution of the RTE has been extended to include Rayleigh scattering with polarization and continuous refraction. The equations have been shown to be well posed when total refraction is ruled out and the numerical method based on “iterations on the source” has been shown to be monotone.

The method is not hard to program and the execution time is a few seconds. The opacity of GHG has a striking effect on the polarization, increased by refraction. Effects on atmospheric temperatures are small but within the precision of the numerical method and it shows that the variations of the refractive index cannot be neglected. Whether this modeling of the atmosphere is sufficient to explain the greenhouse effect of CO_2 is debatable and left to the climatologist (see for example Dufresne et al.(2020)[4]).

Generalization to 3D as in (Hecht et al. (2022)[6]) and (Pironneau-Tournier (2023)[11]) for a non-stratified atmosphere looks possible.

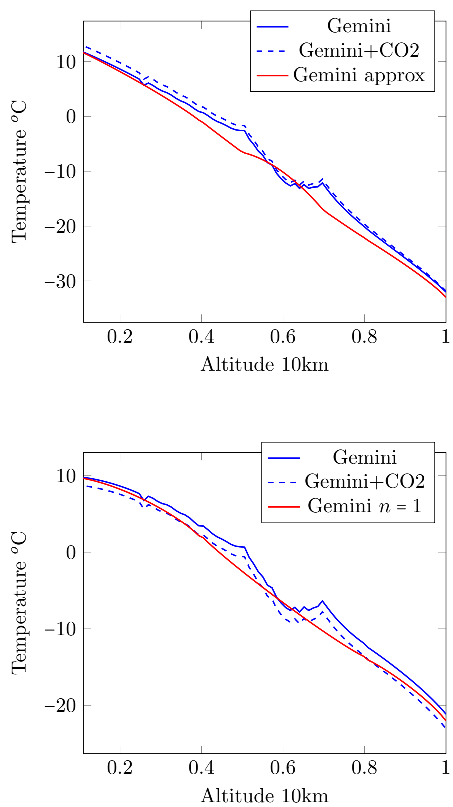

Figure 7: **Case 1** (top) & **Case 2** (bottom). Temperature versus altitude. The dashed curve is computed with κ_1 to account for CO_2.

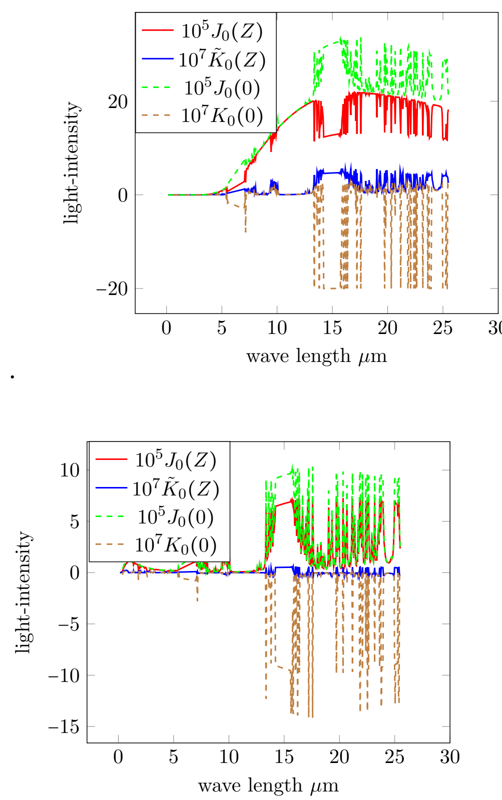

Figure 8: **Case 1** (top) & **Case 2** (bottom) with κ. Total light intensity J_0 and polarized K_0 versus wave length at ground level and altitude 10km.

.

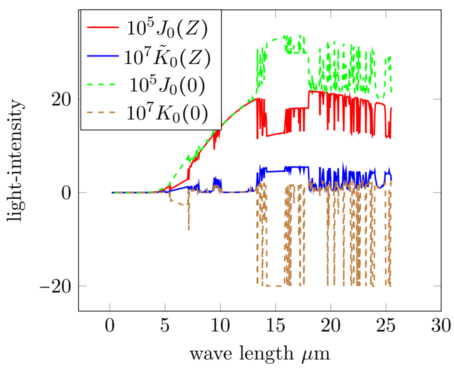

Figure 9: **Case 1** with κ_1. Total light intensity J_0 and polarized K_0 versus wave length at ground level and altitude 10km.

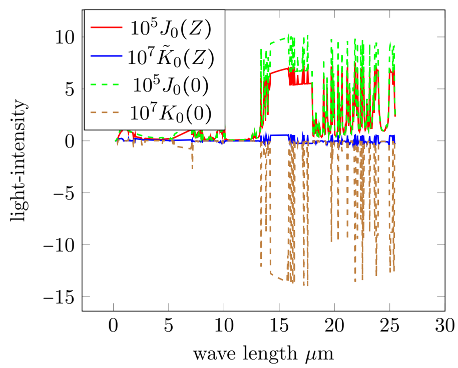

Figure 10: **Case 2** with κ_1. Total light intensity J_0 and polarized K_0 versus wave length at ground level and altitude 10km.

7. Appendix: General Rayleigh scattering Matrix

According to equation (219) in [3]p42 we may express the phase-matrix in the form

$$\boldsymbol{P}\left(\mu,\varphi;\mu',\varphi'\right) = \boldsymbol{Q}[P^0 + (1-\mu^2)\frac{1}{2}(1-\mu')^{\frac{1}{2}}\boldsymbol{P}^{(1)} + \boldsymbol{P}^{(2)}\left(\mu,\varphi;\mu',\varphi'\right)]$$

$$\boldsymbol{Q} = \begin{pmatrix} 1 & 0 & 0 & 0 \\ 0 & 1 & 0 & 0 \\ 0 & 0 & 2 & 0 \\ 0 & 0 & 0 & 2 \end{pmatrix} \quad P^0 = \tfrac{3}{4}\begin{pmatrix} 2\left(1-\mu^2\right)\left(1-\mu'^2\right)+\mu^2\mu'^2 & \mu^2 & 0 & 0 \\ \mu'^2 & 1 & 0 & 0 \\ 0 & 0 & 0 & 0 \\ 0 & 0 & 0 & \mu\mu' \end{pmatrix},$$

$$\boldsymbol{P}^{(1)} = \tfrac{3}{4}\begin{pmatrix} 4\mu\mu'\cos\left(\varphi'-\varphi\right) & 0 & 2\mu\sin\left(\varphi'-\varphi\right) & 0 \\ 0 & 0 & 0 & 0 \\ -2\mu'\sin\left(\varphi'-\varphi\right) & 0 & \cos\left(\varphi'-\varphi\right) & 0 \\ 0 & 0 & 0 & \cos\left(\varphi'-\varphi\right) \end{pmatrix}$$

$$\boldsymbol{P}^{(2)} = \tfrac{3}{4}\begin{pmatrix} \mu^2\mu'^2\cos 2\left(\varphi'-\varphi\right) & -\mu^2\cos 2\left(\varphi'-\varphi\right) & \mu^2\mu'\sin 2\left(\varphi'-\varphi\right) & 0 \\ -\mu'^2\cos 2\left(\varphi'-\varphi\right) & \cos 2\left(\varphi'-\varphi\right) & -\mu'\sin 2\left(\varphi'-\varphi\right) & 0 \\ -\mu\mu'^2\sin 2\left(\varphi'-\varphi\right) & \mu\sin 2\left(\varphi'-\varphi\right) & \mu\mu'\cos 2\left(\varphi'-\varphi\right) & 0 \\ 0 & 0 & 0 & 0 \end{pmatrix},$$

References

[1] M. Ament, C. Bergmann, and D. Weiskopf. Refractive radiative transfer equation. *ACM Transactions on Graphics*, 33(2):2, March 2014.

[2] H. Bussey and G. Birnbaum. Measurement of variations in atmosphereic refractive index xith an airpborne microwave refractometer. *Jornal of National Research of the National Bureau of Standards*, 51(4):171–178, 1953.

[3] S. Chandrasekhar. *Radiative Transfer*. Clarendon Press, Oxford, 1950.

[4] J. Dufresne, V. Eymet, C. Crevoisier, and J. Grandpeix. Greenhouse effect: The relative contributions of emission height and total absorption. *Journal of Climate, American Meteorological Society*, 33(9):3827–3844, 2020.

[5] R. Garcia. Boundary and interface conditions for polarized radiation transport in a multilayer medium. In American Nuclear Society, editor, *International Conference on Mathematics and Computational Methods Applied to Nuclear Science and Engineering*, volume ISBN 978-85-63688-00-2, 2011.

[6] F. Golse, F. Hecht, O. Pironneau, D. Smetz, and P.-H. Tournier. Radiative transfer for variable 3d atmospheres. *J. Comp. Physics*, 475(111864):1–19, 2023.

[7] F. Golse and O. Pironneau. Stratified radiative transfer in a fluid and numerical applications to earth science. *SIAM Journal on Numerical Analysis*, 60(5):2963–3000, 2022.

[8] O. Lehtikangas, T. Tarvainen, A.-D. Kim, and S.-R. Arridge. Finite element approximation of the radiative transport equation in a medium with piece-wise constant refractive index. *Journal of Computational Physics*, 282:345–359, 2015.

[9] L.-H. Liu. Finite volume method for radiation heat transfer in graded index medium. *Journal Of Thermophysics And Heat Transfer*, 20(1):59–66, Jan 2006.

[10] O. Pironneau. Numerical simulation of polarized light with rayleigh scattering in a stratified atmosphere. *Pure and Applied Functional Analysis*, special issue dedicated to Luc Tartar, 2024.

[11] O. Pironneau and P.-H. Tournier. Reflective conditions for radiative transfer in integral form with h-matrices. *Journal of Computational Physics*, 495(112531):1–14, 2023.

[12] G. Pomraning. *The equations of Radiation Hydrodynamics*. Pergamon Press, NY, 1973.

[13] G. Pomraning and B. Ganapol. Simplified radiative transfer for combined rayleigh and isotropic scattering. *The Astrophysical Journal*, 498:671–688, 1998.